nature neuroscience

Direct measurement of somatic voltage clamp errors in central neurons

Stephen R Williams[1] & Simon J Mitchell[1]

The somatic voltage clamp technique has revolutionized understanding of synaptic physiology and the excitability of neurons. Although computer simulations have indicated that the somatic voltage clamp poorly controls voltage in the dendritic tree of neurons, where the majority of synaptic contacts are made, there has not been an experimental description of the performance of the somatic voltage clamp. Here, we directly quantify errors in the measurement of dendritic synaptic input by the somatic voltage clamp using simultaneous whole-cell recordings from the soma and apical dendrite of rat neocortical pyramidal neurons. The somatic voltage clamp did not control voltage at sites other than the soma and distorted measurement of the amplitude, kinetics, slope conductance and reversal potential of synaptic inputs in a dendritic distance–dependent manner. These errors question the use of the somatic voltage clamp as a quantitative tool in dendritic neurons.

Central neurons receive the vast majority of excitatory and inhibitory synaptic input at dendritic sites, where synaptic potentials are shaped by interaction with voltage-activated ion channels before reaching the soma and axon[1]. Detailed information about the function of dendritic synapses and the macroscopic properties of voltage-activated ion channels has come from the use of electrophysiological recording techniques. However, electrophysiological recordings are typically made from the soma, and consequently the properties of dendritic synapses and ion channels have been observed indirectly. Over the last thirty years, the somatic voltage clamp technique has become the approach of choice to investigate synaptic physiology and neuronal excitability *in vitro* and *in vivo*[2–8]. Despite the widespread use of the somatic voltage clamp, little attention has been focused on its limitations. Pioneering theoretical studies have suggested that the voltage clamp does not uniformly control voltage throughout the soma and dendritic tree of model neurons and thus may be expected to distort the electrical measurement of dendritic synapses and ion channel activity[7,9–11]. However, there has not been a direct experimental description of the magnitude of such distortions, mainly because of the technical difficulties imposed by electrical recording from dendrites. Here, we use multisite whole-cell recordings from the soma and dendrites to test the performance of the somatic voltage clamp experimentally in a class of neocortical pyramidal neurons maintained in brain slices under a variety of experimental conditions.

RESULTS

Ideally, the somatic voltage clamp should uniformly control the membrane potential of a neuron and accurately measure the amplitude and time course of synaptic currents generated throughout the dendritic tree. How far does the operation of the somatic voltage clamp deviate from this ideal in practice? To assess the utility of the somatic voltage clamp experimentally, we made triple whole-cell recordings from rat layer 5 pyramidal neurons maintained in brain slices. Synaptic input was stimulated at defined somatic or apical dendritic sites with a real-time dynamic clamp[12]. We used independent, closely spaced whole-cell pipettes to inject current and record membrane potential, allowing the generation and recording of simulated synaptic conductance undistorted by resistive and capacitive artifacts associated with single-electrode whole-cell recording[12,13]. At the soma, a simultaneous whole-cell recording was used to measure synaptic current under voltage clamp or synaptic potentials under current clamp. This configuration allowed a direct comparison of the amplitude and time course of synaptic current recorded from the dendritic site of generation and from the soma under voltage clamp. Furthermore, the deviation from uniform voltage control was measured by recording the magnitude of voltage escape at the site of generation of simulated synapses (**Fig. 1**).

First, we tested the operation of the voltage clamp in neurons recorded at near-physiological temperature following the formation of low–series resistance somatic whole-cell recordings using an intrapipette solution designed to maintain 'normal' electrical properties (series resistance = 10.0 ± 0.4 MΩ; $n = 23$; 35–37 °C)[12,13]. The series resistance associated with the formation of the somatic whole-cell recording was electronically compensated for by >90%, unless otherwise stated. When we generated a simulated excitatory postsynaptic conductance (dEPSC) at the soma, or from perisomatic sites, the somatic voltage clamp recovered a large fraction of the injected synaptic current (measured at peak amplitude, **Fig. 1a**,**c**,**d**). In contrast, when we generated dEPSCs from progressively remote apical dendritic sites, the voltage clamp underestimated the amplitude of synaptic inputs, reporting only a small fraction of the injected

[1]Medical Research Council Laboratory of Molecular Biology, Hills Road, Cambridge CB2 0QH, UK. Correspondence should be addressed to S.R.W. (srw@mrc-lmb.cam.ac.uk).

Received 24 January; accepted 12 May; published online 15 June 2008; doi:10.1038/nn.2137

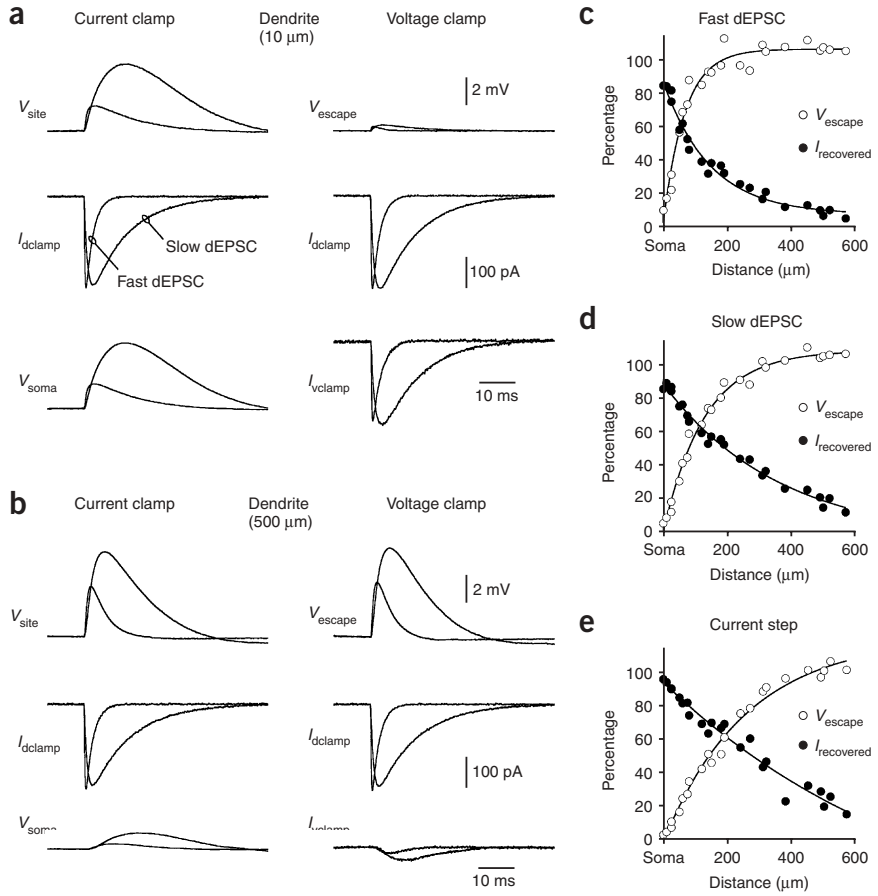

Figure 1 The somatic voltage clamp does not control dendritic simulated EPSCs at near-physiological temperatures (35–37 °C). All voltage clamp recordings used >90% series resistance compensation. (**a**) The somatic voltage clamp adequately controls perisomatically generated simulated excitatory postsynaptic conductance (dEPSCs) (I_{dclamp}), recovering a large fraction of the injected synaptic current (I_{vclamp}) and maintaining good voltage control, as shown by the minimal recorded escape voltage (V_{escape}). (**b**) The somatic voltage clamp recovers only a small fraction of dendritic synaptic current and does not control the membrane potential, as shown by the similarity between EPSPs recorded at the dendritic site of generation under current clamp (V_{site}) and the dendritic escape voltage under voltage clamp. (**c**–**e**) Quantification of the distance-dependent loss of recovered synaptic current and dendritic voltage control when synaptic inputs were generated from apical dendritic sites. Recovered current ($I_{recovered}$) represents percentage of injected current, and dendritic voltage escape (V_{escape}) represents percentage of the amplitude of EPSPs recorded under current clamp at the dendritic site of generation. Data are shown for dEPSCs with fast and slow kinetics and in response to a current step (–100 pA, 30 ms) and have been fit with single exponential functions (lines).

synaptic current (**Fig. 1b–d**). This distance-dependent attenuation was greatest for dEPSCs that replicated the fast time course of spontaneous EPSCs in layer 5 pyramidal neurons[13,14], with the somatic voltage clamp recovering only 50% of the amplitude of fast dEPSCs generated just 90 μm from the soma, a distance that represents only one-tenth of the apical dendritic tree[15] (fast dEPSC time course: $\tau_{rise} = 0.2$ ms, $\tau_{decay} = 2$ ms; $E_{EPSC} = 0$ mV; $g_{EPSC} = 4.5$ nS; **Fig. 1a–c**). In response to dEPSCs with a time course five times slower, 50% of the amplitude of slow dEPSCs was recovered at 195 μm from the soma, suggesting that the performance of the somatic voltage clamp was frequency dependent (slow dEPSC time course: $\tau_{rise} = 1$ ms, $\tau_{decay} = 10$ ms; **Fig. 1a,b,d**). To further test this idea, we injected a step of negative DC current at somatic or dendritic sites (–100 pA, 30 ms). The voltage clamp recovered 50% of the injected current at 277 μm from the soma (**Fig. 1e**). These frequency-dependent properties were not governed by the responsiveness of the instrumentation, as the voltage clamp accurately measured fast dEPSCs when connected to an artificial resistive-capacitive network that modeled the properties of an isopotential passive neuron (**Supplementary Fig. 1** online).

The inability of the somatic voltage clamp to measure dendritic synaptic input accurately is therefore shaped by the electrotonic structure of the neuron, where dendritic synaptic currents are progressively filtered by the resistive and capacitive properties of the dendritic membrane[13,16–18]. Consistent with this idea, the distance- and frequency-dependent distortion of synaptic current was mirrored by an inability of the somatic voltage clamp to control the membrane potential at dendritic sites. Ideally, the voltage clamp should control the membrane potential at a fixed value throughout the time course of a synaptic conductance, as escape from voltage control distorts the amplitude and kinetics of the measured synaptic current. However, in practice, the somatic voltage clamp did not control the membrane potential at the dendritic site of dEPSC generation (**Fig. 1**). Notably, in response to fast dEPSCs, voltage control at the dendritic site of generation was totally lost ~180 μm from the soma, with 50% of voltage control lost at just 41 μm (**Fig. 1a–c**). At apical dendritic sites distal to 180 μm, the amplitude of excitatory postsynaptic potentials (EPSPs) generated in response to the injected dEPSC were of similar amplitude when the somatic recording amplifier was set in either voltage or current clamp configuration, indicating that the membrane potential was uncontrolled during the synaptic conductance (**Fig. 1b–d**). The spatial profile of voltage control was shaped by the kinetics of the input signal (**Fig. 1**). Notably, in response to a DC current step, complete loss of voltage control occurred ~400 μm from the soma (50% point = 145 μm; **Fig. 1e**). Thus, even at steady state, the somatic voltage clamp did not control voltage through the majority of the dendritic tree.

If the voltage clamp functions poorly under conditions of near-optimal series resistance (R_S) compensation, how well does it function in the absence of R_S compensation, a commonly used recording configuration? Direct comparison showed that R_S compensation was critical to the ability of the voltage clamp to control voltage and recover synaptic current generated at perisomatic sites (**Supplementary Fig. 2** online). In the absence of R_S compensation, only 44% of the peak amplitude of somatically generated fast dEPSCs was recovered, and 54% of voltage control was lost (**Supplementary Fig. 2**). Consequently, in the absence of R_S compensation, the neuron was not voltage clamped, leading to massive errors in the measurement of the amplitude of dendritic dEPSCs ($n = 23$; **Supplementary Fig. 2b,c**).

Can the performance of the somatic voltage clamp be improved? Voltage clamp experiments conducted on isolated neurons and those maintained in brain slices are often made at room temperature in order to slow the time course of synaptic currents and increase neuronal

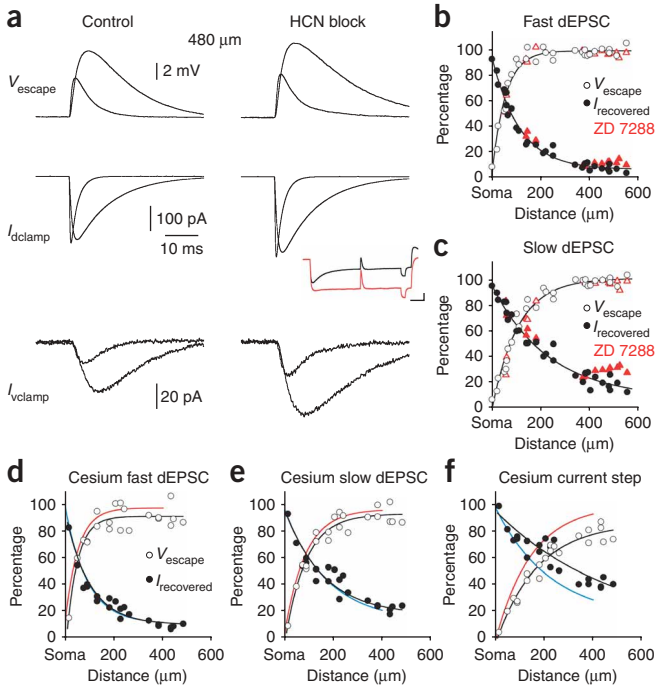

Figure 2 Somatic voltage clamp errors at room temperature (24–25 °C). (**a**) The somatic voltage clamp does not control dEPSCs generated from dendritic sites at room temperature (left), as shown by the large dendritic voltage escape and distortion of somatically recovered synaptic current. The blockade of I_H by the bath application of ZD 7288 (20 μM) causes only a minor improvement in the performance of the voltage clamp (right). The inset shows the block of voltage sag at the dendritic site by ZD 7288 (red trace), and scale bars represent 3 mV and 100 ms. (**b**,**c**). Summary data illustrating the steep distance-dependent reduction of the percentage of injected synaptic current recovered by the somatic voltage clamp and increase in percentage voltage escape for fast and slow dEPSCs. The red symbols represent results obtained in ZD 7288 (open triangles: voltage escape in ZD 7288; filled triangles: recovered current in ZD 7288). (**d**–**f**) Distance-dependent measurement errors of current and voltage escape in neurons recorded with cesium-filled pipettes at room temperature. Data are summarized as in **b** and **c**. Colored lines refer to measurement errors of current (blue) and voltage escape (red) in cesium-dialyzed neurons recorded at near-physiological temperatures.

input resistance[19]. In addition, the leak and resting conductance of a neuron can be reduced pharmacologically, which should increase membrane resistance and thus lessen the effects of the electrical filtering of synaptic input[17]. We tested each of these conditions.

First, we examined the performance of the voltage clamp at room temperature (24–25 °C; series resistance = 12.0 ± 0.4 MΩ; $n = 30$; **Fig. 2**). The use of the dynamic clamp allowed independent investigation of the influence of preparation temperature on the electrical properties of the neuron and the impact of synaptic kinetics. Initially, we generated fast and slow dEPSCs with kinetics identical to those used at physiological temperatures. At room temperature, the somatic voltage clamp recovered 94% of synaptic current when we generated fast dEPSCs at the soma, but markedly underestimated the magnitude of apical dendritic synaptic current, such that a 50% measurement error was apparent at 80 μm from the soma (**Fig. 2a**,**b**). Similarly, the magnitude of voltage escape at the peak of dendritic fast dEPSCs was marked, reaching 50% at just 37 μm from the soma. At room temperature, the performance of the voltage clamp was frequency dependent, with 50% measurement errors found at 165 and 270 μm from the soma for slow dEPSCs and DC current steps, respectively (**Fig. 2c**). Next, we slowed the kinetics of the simulated synaptic inputs by a factor of 3 to model the influence of a 10 °C decrease in temperature on the properties of postsynaptic currents[19]. Thus, at room temperature, the kinetics of fast dEPSCs had rise and decay time constants of 0.6 and 6 ms, respectively, and are referred to as rt-fast dEPSCs. Measurement errors associated with rt-fast dEPSCs were large, with 50% of dendritic synaptic current recovered at 140 μm and 50% of voltage control lost at 60 μm. Similarly, when the kinetics of slow dEPSCs were slowed by a factor of 3 to yield rise and decay time constants of 3 and 30 ms, respectively, the somatic voltage clamp recovered 50% of dendritic synaptic current at 245 μm, and 50% of voltage control was lost at 120 μm from the soma (**Supplementary Fig. 3** online). Taken together, these data indicate that slowing of the kinetics of synaptic currents improves the performance of the somatic voltage clamp and suggest that synaptic inputs activating postsynaptic receptor mechanisms that generate fast or slow synaptic conductance, such as the activation of AMPA and NMDA receptors[20], cannot be considered to be equally controlled. To illustrate this, we slowed the kinetics of dEPSCs by a factor of 7.5 and found that this shifted the site within the dendritic tree where a 50% measurement error of synaptic current was apparent by 140 μm (**Supplementary Fig. 3**). This frequency-dependent distortion should, therefore, be considered when analyzing the AMPA/NMDA ratio of excitatory synapses in dendritic neurons.

Is the performance of the voltage clamp improved by recording at room temperature and by pharmacologically reducing resting conductance? In layer 5 pyramidal neurons, the non-inactivating inward current I_H forms the major resting conductance[21,22]. I_H channels are nonuniformly distributed and are expressed at high density in the apical dendritic arbor[21–23]. Consequently, the pharmacological blockade of I_H has been shown to decrease the attenuation of synaptic potentials as they spread through the apical dendritic tree of layer 5 pyramidal neurons[21,22,24]. The bath application of ZD 7288 blocked I_H and had a site-dependent influence on the performance of the somatic voltage clamp (20 μM; $n = 14$; **Fig. 2a**, inset). When we generated dEPSCs from somatic or proximal dendritic sites, the block of I_H had little effect on the somatic measurement of synaptic current (**Fig. 2b**,**c**). However, when we generated dEPSCs from distal dendritic sites, the application of ZD 7288 significantly increased the peak amplitude of the somatically measured synaptic current (480 ± 16 μm from the soma; control fast dEPSC: 8.2 ± 0.9%; ZD 7288: 12.5 ± 0.6%; $P < 0.001$; control slow dEPSC: 19.4 ± 1.7%; ZD 7288: 29.7 ± 0.7%; $P < 0.001$; $n = 7$; **Fig. 2a–c**). It should be noted that, although this improvement was significant, the somatic voltage clamp recovered only a small fraction of synaptic current from and failed to control voltage at distal dendritic sites when we blocked I_H (voltage escape: fast dEPSC: control: 100.9 ± 1.5%; ZD 7288: 97.4 ± 0.6%; slow dEPSC: control: 100.0 ± 1.4%; ZD 7288: 97.0 ± 1.0%; **Fig. 2a–c**).

Many whole-cell voltage clamp recordings are made with pipettes filled with a cesium-based solution to reduce resting and leak conductance pharmacologically. To investigate the influence of this, we filled both somatic and dendritic recording pipettes with a cesium-based solution (see Methods). Under these conditions, the measurement of dendritic synaptic currents was not improved either at room temperature or at near-physiological temperatures (**Fig. 2d–f**). At room temperature, the somatic voltage clamp recorded only 50% of the amplitude of fast dEPSCs generated at dendritic sites 74 μm from the soma, and 50% of voltage control was lost at just 43 μm from the soma (**Fig. 2d**; $n = 21$; series resistance = 13 ± 1 MΩ). In response to a step of dendritic DC current (–100 pA, 30 ms), we noted a 50% measurement error when we generated current steps 340 μm from the soma, and 50%

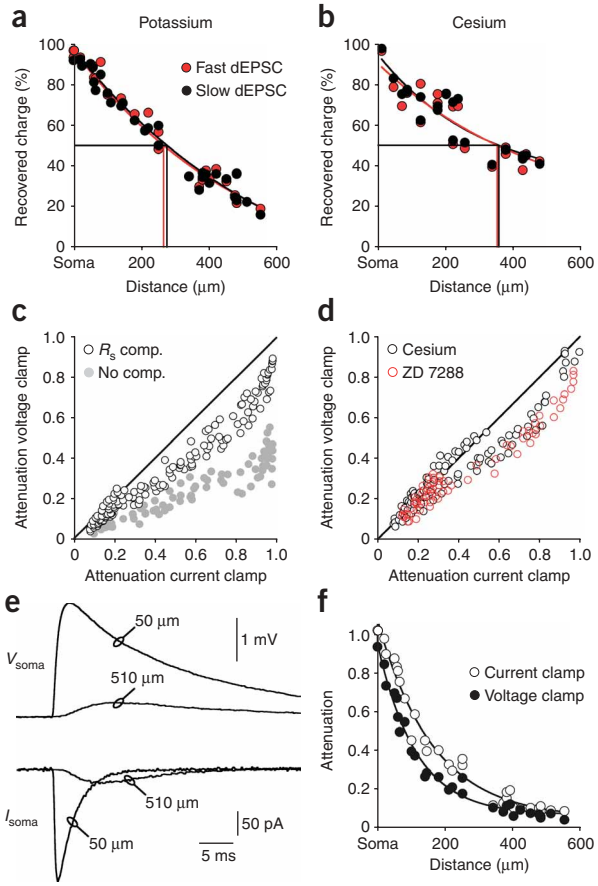

Figure 3 Somatic recovery of dendritic synaptic charge. (**a**) Distance-dependent attenuation of synaptic charge. Attenuation represents the fraction of the integral of dendritic dEPSC recorded from the soma of layer 5 pyramidal neurons using a potassium-based pipette-filling solution at room temperature. (**b**) Dendro-somatic attenuation of synaptic charge recorded with electrodes filled with a cesium-based solution. Lines through data in **a** and **b** represent exponential fits, and drop lines show 50% attenuation points. (**c**) Ratio of the dendro-somatic attenuation of the peak amplitude of synaptic events recorded from the dendritic site of generation and the soma under current and voltage clamp, in the presence and absence of series resistance (R_s) compensation. Larger fractions refer to events generated from proximal dendritic sites. (**d**) Attenuation ratio under voltage and current clamp for recordings made with a cesium-based pipette solution and those made with a potassium-based solution after the blockade of I_H with ZD 7288. (**e**) Comparison of the amplitude and waveform of synaptic potentials and currents recorded from the soma under current (V_{soma}) and voltage clamp (I_{soma}); dEPSCs were generated at the indicated dendritic sites. (**f**) Spatial profile of dendro-somatic attenuation of fast dEPSCs recorded under current and voltage clamp. Data are fit with single exponential functions (lines).

of voltage control was lost at 157 μm. However, steady-state voltage control of distal apical dendritic sites was significantly improved when we dialyzed neurons with cesium (cesium: 445 ± 12 μm, voltage escape 78.8 ± 3.6%, $n = 4$; potassium: 480 ± 16 μm, voltage escape 94.5 ± 1.3%, $n = 7$; $P < 0.02$). When we made recordings at near-physiological temperatures with cesium-filled electrodes, the measurements of the amplitude and the voltage control of dendritic dEPSCs were heavily distorted, as was the measurement of current steps (**Fig. 2e–f**, fit to $n = 19$ points; distribution shown in **Supplementary Fig. 4** online). Therefore, the pharmacological reduction of resting and leak conductance by the intracellular diffusion of cesium from somatic and dendritic patch pipettes does little to improve the measurement of synaptic currents by the somatic voltage clamp.

These data demonstrate that the somatic voltage clamp inaccurately measures the amplitude of dendritic synaptic currents. However, the use of the dynamic clamp allowed analysis of another key parameter of synaptic efficacy, the charge transferred from the dendritic site of dEPSC generation to the soma (**Fig. 3a,b**). When we recorded neurons with pipettes filled with a potassium-based solution at room temperature, the dendro-somatic attenuation of synaptic charge was severe, with 50% attenuation occurring for dendritic fast and slow dEPSCs generated ~270 μm from the soma (**Fig. 3a**). In contrast, when we dialyzed neurons with cesium, the fraction of dendritic dEPSC charge recovered at the soma was substantially greater, with 50% attenuation occurring ~365 μm from the soma (**Fig. 3b**). The dichotomy between the distance-dependent attenuation of the amplitude of dEPSCs and their charge prompted us to compare the relationship between the attenuation of synaptic currents recorded under somatic voltage clamp and synaptic potentials recorded under somatic current clamp (**Fig. 3c–f**). When we recorded neurons at room temperature using potassium-filled pipettes and compensated for series resistance, dendro-somatic attenuation of dEPSCs generated widely across the apical dendritic tree was greater under voltage clamp across a broad range of dEPSC properties (τ_{rise}: 0.2–1 ms in 0.2-ms intervals; τ_{decay}: 2–10 ms in 2-ms intervals; **Fig. 3c**). The distortion imposed under voltage clamp was exacerbated if the series resistance of the somatic recording was uncompensated (**Fig. 3c**). When we dialyzed neurons with cesium or pharmacologically blocked I_H, dendro-somatic attenuation was also greater under voltage clamp (**Fig. 3d**). The shape of these relationships helps explain the factors governing the description of dendritic synaptic currents by the somatic voltage clamp. As the somatic voltage clamp poorly controlled synaptic currents at their dendritic site of generation, the amplitude and time course of somatically recorded synaptic currents may be determined primarily by the size and shape of synaptic potentials as they spread from a dendritic site of generation toward the soma. Direct comparison showed that distance-dependent filtering of the amplitude and time course of synaptic potentials corresponded well with that of synaptic currents (**Fig. 3e**). Similarly, pooled data showed that the shape of the curve describing the dendro-somatic attenuation of synaptic currents followed that of synaptic potentials recorded under current clamp (**Fig. 3f**). These data suggest that the somatic voltage clamp largely clamps only the synaptic potential apparent at or near the soma.

How are other properties of dendritic synaptic input, such as kinetics, conductance and reversal potential distorted by the somatic voltage clamp when recordings are made at room temperature? Simultaneous recording allowed direct comparison of the rise and decay kinetics of dEPSCs at the dendritic site of generation with those measured from the soma under voltage clamp. When we generated dEPSCs from the soma, the voltage clamp accurately reported their kinetic properties (**Fig. 4a**). However, errors in the measurement of these parameters increased markedly when we generated dEPSCs from apical dendritic sites, with the somatic voltage clamp reporting rise times sevenfold slower and half-widths fourfold slower than those at the dendritic site of fast dEPSC generation 400 μm from the soma (**Fig. 4a**). The blockade of I_H did not improve the description of dendritic dEPSC kinetics by the somatic voltage clamp (**Fig. 4a**). Furthermore, distance-dependent errors in the measurement of dEPSC kinetics were as great, if not greater, when we dialyzed neurons with cesium (**Fig. 4b**).

Simultaneous recording allowed quantification of the errors associated with dendritic voltage escape. Direct recording showed that dendritic EPSPs were generated as a consequence of the escape from

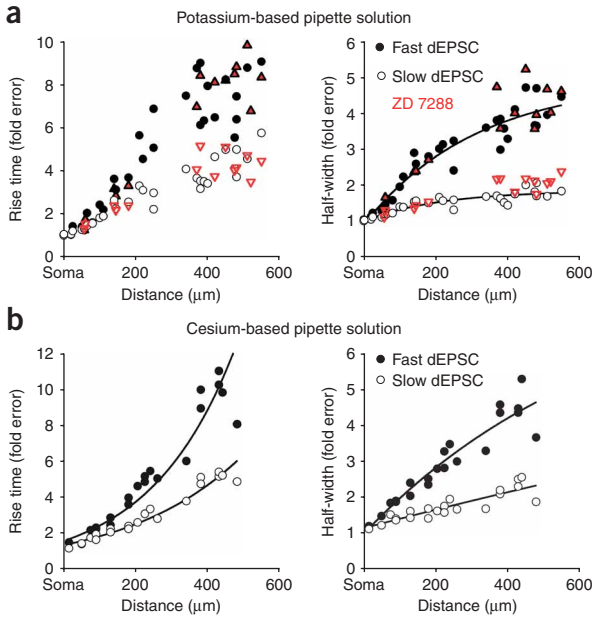

Figure 4 The somatic voltage clamp inaccurately measures the kinetics of dendritic synaptic currents at room temperature. (**a**) The somatic voltage clamp inaccurately reports the 10–90% rise time and half-width of dendritic dEPSCs. Values are expressed as fold error relative to those measured at the dendritic site of dEPSC generation, where an error of 1 indicates identical values at somatic and dendritic sites. Recordings were made at room temperature with pipettes filled with a potassium-based solution (black symbols) and after the blockade of I_H with ZD 7288 (red filled triangles: fast dEPSCs in ZD 7288; red open triangles: slow dEPSCs in ZD 7288). (**b**) Distance-dependent distortion of the somatic measurement of the rise time and half-width of dendritic dEPSCs recorded at room temperature with cesium-filled electrodes. Lines represent single exponential fits.

voltage clamp (**Figs. 1**, **2** and **5**). Unclamped dendritic EPSPs lagged the injected synaptic current because of the time taken to charge the dendritic membrane (**Fig. 5a**). Consequently, we recorded greater voltage escape at the peak of slow dEPSCs (**Fig. 5a**). Because voltage escape decreased the driving force for the excitatory conductance, errors in injected synaptic current were greatest for slow synaptic inputs, in contrast with other measurement errors (**Fig. 5b**). The reduction of injected synaptic current increased in a distance-dependent manner because of the declining ability of the somatic voltage clamp to control the dendritic membrane potential (**Fig. 5b**). Notably, as we increased the conductance of simulated synaptic, errors of injected synaptic current also increased, because voltage escape at the peak of larger synaptic currents was greater owing to the faster charging of the dendritic membrane potential (**Fig. 5c**). The magnitude of such errors increased as synaptic inputs were generated more distally in the dendritic tree (**Fig. 5c**, inset). Thus, the escape from somatic voltage control introduces an erroneous distance-dependent nonlinearity to the magnitude of dendritic synaptic current.

The lack of dendritic voltage control should also influence the somatically recorded reversal potential of dendritic synaptic inputs and thus the ability to separate and quantify excitatory and inhibitory synaptic conductance under somatic voltage clamp. To investigate this, we generated simulated inhibitory postsynaptic conductances (dIPSCs) at defined somatic or apical dendritic sites (dIPSC time course: τ_{rise} = 1 ms, τ_{decay} = 10 ms; E_{IPSC} = –80 mV; g_{IPSC} = 18 nS; n = 16; **Fig. 6a**). The somatic membrane potential was stepped across a 50-mV range under voltage clamp. Independent recording confirmed that the somatic voltage was well controlled (**Fig. 6a**, inset). Therefore, when we generated dIPSCs at the soma, the voltage clamp accurately reported the reversal potential and peak slope conductance of the inhibitory synaptic input, calculated by linear regression (**Fig. 6a**). In contrast, when we generated dIPSCs at apical dendritic sites, the dendritic membrane potential was inaccurately controlled (**Fig. 6a**). Consequently, when we calculated the reversal potential and slope conductance of dendritic dIPSCs with respect to the somatic membrane potential and voltage clamp current, we found marked distance-dependent distortions (**Fig. 6b**,**c**). However, at dendritic sites of generation, the reversal potential and slope conductance of dIPSCs were stationary when calculated with respect to the locally recorded membrane potential and current (**Fig. 6c**). We found similar errors when we calculated the reversal potential and slope conductance of dendritic dEPSCs from somatically recorded voltage and current (dEPSC time course: τ_{rise} = 0.5 ms, τ_{decay} = 5 ms; E_{EPSC} = 0 mV; g_{EPSC} = 4.5 nS: calculated reversal potential: somatic dEPSC: 3 mV; distal dendritic dEPSC at 439 ± 20 μm from soma; 443 ± 87 mV; n = 5; **Fig. 6b**). As recordings with electrodes filled with a cesium-based solution improved steady-state voltage control at distal dendritic sites, we explored if the description of the reversal potential of synaptic currents also improved. Recording with cesium-filled pipettes improved the measurement accuracy of the reversal potential of dIPSCs and dEPSCs generated from distal apical dendritic sites (**Fig. 6d** and **Supplementary Fig. 5** online). However, cesium dialysis did not improve the measurement of the slope conductance of synaptic currents (**Supplementary Fig. 5**). Consistent with these findings, the pharmacological block of I_H decreased errors in the somatic

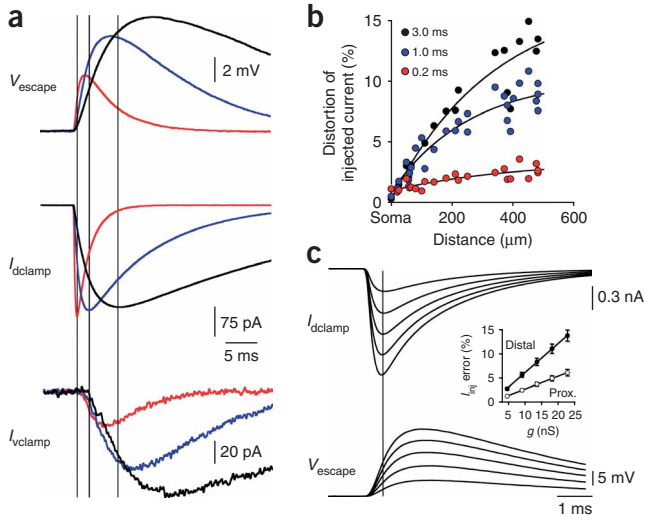

Figure 5 Dendritic voltage escape influences injected synaptic current. (**a**) Simultaneous recording of voltage escape at the site of dEPSC generation (480 μm from the soma), dendrite-injected synaptic current and somatic voltage clamp current at room temperature. Vertical lines correspond to the peak of the injected synaptic current. Colored traces refer to dEPSCs with τ_{rise} of 0.2 (red), 1.0 (blue) and 3.0 ms (black). (**b**) Voltage escape leads to a distance-dependent distortion of the value of injected synaptic current. Values are expressed as percentage error from the ideal (zero voltage escape) case. This error is dependent on the kinetics of the dEPSC. (**c**) Relationship between the magnitude of synaptic conductance and dendritic voltage escape. At the peak of the synaptic current (vertical line), voltage escape increases with the magnitude of synaptic conductance. The inset shows pooled data describing the relationship between errors in injected current for dEPSCs of increasing magnitude generated at proximal (45 ± 10 μm; n = 8) and distal apical dendritic sites (461 ± 12 μm; n = 5). Values represent mean ± s.e.m.

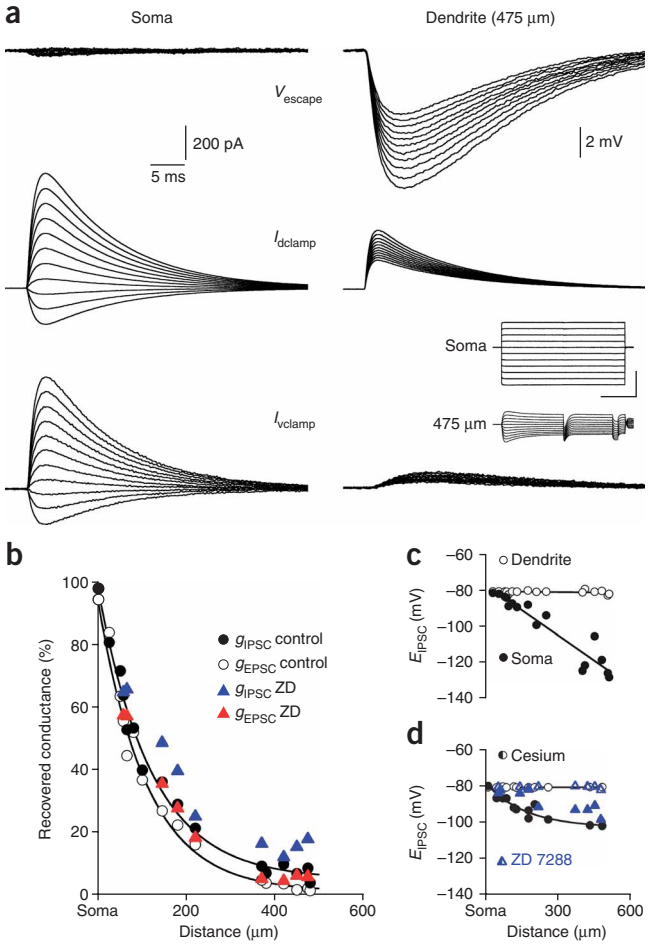

Figure 6 Distortions of reversal potential and slope conductance. (**a**) A family of simulated inhibitory synaptic conductances (V_{rev} = –80 mV) generated from the soma (left) or from a distal apical dendritic site (475 µm from the soma, right). During triple somatic recording, the recovered somatic voltage clamp current (I_{vclamp}) corresponds well with the injected current (I_{dclamp}). Somatic dIPSCs were recorded across a range of holding potentials (–93 to –43 mV, 5-mV increments, inset, soma) and reverse close to –80 mV. In contrast, when inputs are generated from a distal apical dendritic site, an identical somatic voltage clamp protocol does not reverse the synaptic current and severely distorts its amplitude owing to poor voltage control at the dendritic site of generation (V_{escape} and inset, 475 µm). Inset scale bars represent 20 mV and 200 ms. (**b**) Summary data describing the percentage error of the somatically recovered conductance of excitatory and inhibitory synaptic inputs generated from apical dendritic sites under control conditions and with ZD 7288. (**c**) The reversal potential of dIPSCs calculated from voltage and current recorded from the soma or dendritic sites. Note the marked distance-dependent distortion of the calculated somatic reversal potential when recordings were made with at room temperature with pipettes filled with a potassium-based solution. (**d**) Calculated somatic and dendritic reversal potential of dIPSCs recorded with cesium-filled pipettes or with potassium-filled pipettes after the blockade of I_H with ZD 7288.

measurement of reversal potential but only marginally increased the recovered slope conductance (potassium filled-pipettes, distal dendritic sites 429 ± 23 µm from soma: control E_{IPSC} = –118 ± 5 mV; ZD 7288 E_{IPSC} = –94 ± 2 mV; control E_{EPSC} = 398 ± 97 mV; ZD 7288 E_{EPSC} = 227 ± 24 mV; n = 4; **Fig. 6b,d**). Taken together, these data suggest that measurement of the reversal potential of dendritic synaptic currents alone cannot be used as an indication of the adequacy of somatodendritic voltage control.

In many neural circuits, synaptic excitation is controlled by feedforward and feedback synaptic inhibition; consequently, during the dynamic operation of neural circuits, excitatory and inhibitory synaptic conductance overlap in time[25–29]. Theoretically, the somatic voltage clamp can be used to separate total synaptic conductance into excitatory and inhibitory components, if the reversal potential of one of the components is known by calculation or by observation[8,25]. Recently, this technique has been used to study the dynamic behavior of neural circuits *in vitro* and *in vivo*[8,25,26,29–31]. To examine how accurately temporally overlapping excitatory and inhibitory synaptic conductance can be separated by the somatic voltage clamp, we generated a sequence of single excitatory and inhibitory synaptic inputs at somatic or apical dendritic sites (dEPSCs lead dIPSCs by 1 ms; dEPSC time course: τ_{rise} = 0.5 ms, τ_{decay} = 5 ms; E_{EPSC} = 0 mV; g_{EPSC} = 4.5 nS; dIPSC time course: τ_{rise} = 1 ms, τ_{decay} = 10 ms; E_{IPSC} = –80 mV; g_{IPSC} = 18 nS; n = 16; **Fig. 7**). When generated at the soma, the somatic voltage clamp accurately measured the total synaptic conductance and allowed precise separation into excitatory and inhibitory components (**Fig. 7a**). However, when we generated the dEPSC-IPSC sequence from apical dendritic sites, the total synaptic conductance was underestimated in a dendritic distance–dependent manner (**Fig. 7**). Although the total conductance of dendritic synaptic input could be separated into excitatory and inhibitory components, there were substantial distortions due to dendritic voltage escape (**Fig. 7a**). Distortions were most evident in excitatory synaptic conductance generated at dendritic sites >200 µm from the soma, where the somatically recovered excitatory conductance had a multiphasic shape, characterized by an early positive followed by a pronounced negative phase (**Fig. 7a**). Consequently, when we calculated the area of somatically recovered excitatory and inhibitory components, excitatory inputs exhibited artifactual net negative conductance (**Fig. 7b**, inset). To explore if the somatic voltage clamp could be used to measure the balance between excitatory and inhibitory synaptic conductance during barrages of synaptic input designed to mimic patterns of synchronized network activity *in vivo* and *in vitro*[8,26,31,32], we generated random trains of excitatory and inhibitory synaptic inputs at dendritic sites (**Fig. 8a**). In response to a barrage of dendritic synaptic input, the

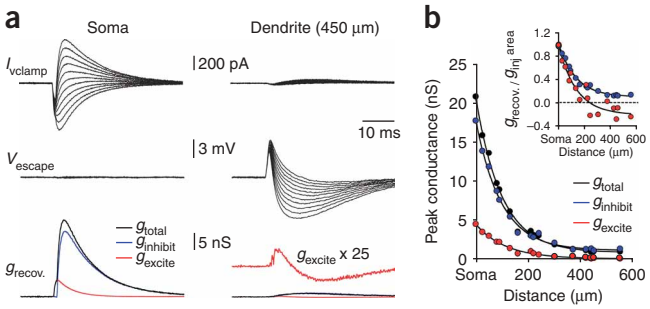

Figure 7 Failure to separate temporally overlapping excitatory and inhibitory dendritic synaptic conductance. (**a**) A family of simulated excitatory and inhibitory synaptic inputs generated with a delay of 1 ms at the soma (left) or from a distal apical dendritic site (450 µm). The lower traces show the recovered total somatic synaptic conductance (black) separated into excitatory (red) and inhibitory (blue) components by linear regression at each sample point. Note the massive distortion of the amplitude and time course of the recovered synaptic conductance when events were evoked from a distal apical dendritic site. (**b**) Summary data describing the marked distance-dependent distortion of the somatically recovered peak synaptic conductance. The inset shows the ratio of the area (nS × ms) of excitatory and inhibitory components recovered from the soma as a fraction of injected synaptic conductance.

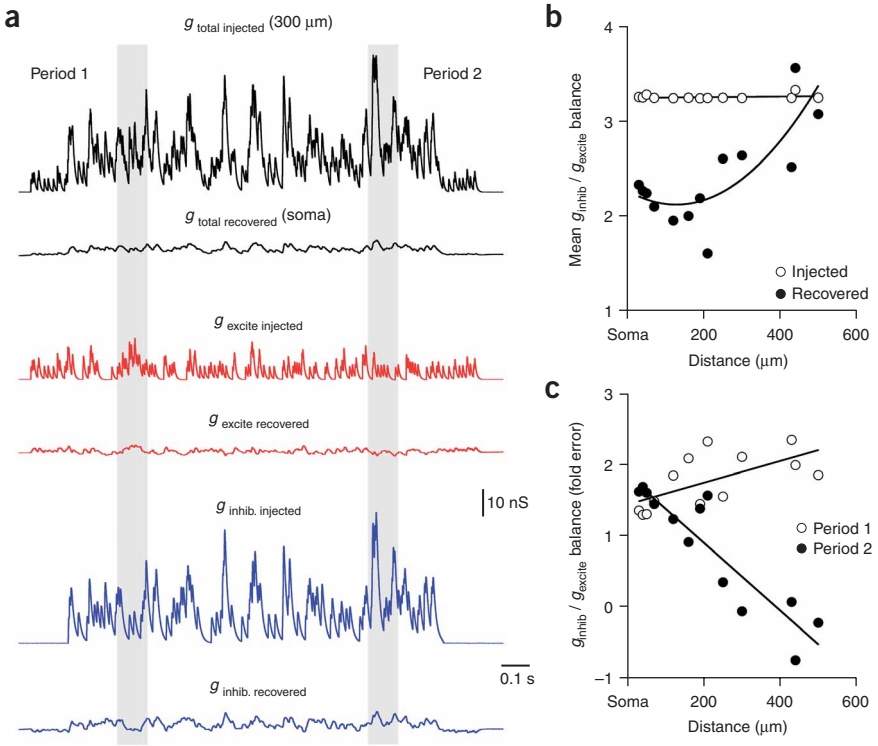

Figure 8 Errors in the measurement of excitation and inhibition during a barrage of dendritic synaptic activity. (**a**) Total synaptic conductance separated into excitatory and inhibitory components by linear regression at the site of generation and the soma. (**b**) Errors in the somatic measurement of the balance between excitatory and inhibitory components. Across the barrage, the mean excitatory-inhibitory balance at site of generation is stationary but is distorted in a nonlinear distance-dependent manner when recovered from the soma. (**c**) During the barrage, the somatic error function is determined by the time-dependent values of excitatory and inhibitory conductance (plot refers to indicated periods in **a**).

somatic voltage clamp underestimated the total dendritic synaptic conductance and poorly estimated the average balance between excitatory and inhibitory components (**Fig. 8a**,**b**). Under these conditions, we did not find a clear relationship between the magnitude of errors and the dendritic site of synapse generation (**Fig. 8b**). However, errors in the measurement of excitatory and inhibitory conductance were critically determined by the time-varying composition of the injected synaptic conductance and were not stationary during the barrage of synaptic input; rather, they varied widely from one time period to another (**Fig. 8c**). Taken together, these data indicate that the amplitude and kinetic properties of temporally overlapping dendritic excitatory and inhibitory synaptic inputs cannot be accurately separated and measured with the somatic voltage clamp.

DISCUSSION

Neurons are anatomically distributed structures, often possessing elaborate dendritic trees that receive the majority of synaptic input[1]. Pioneering theoretical studies have shown that dendrites act as electrical filters, progressively attenuating the amplitude and slowing the time course of synaptic potentials as they spread from dendritic site of generation to the soma[16]. Direct dendritic recording techniques have experimentally confirmed and quantified the extent of such cable filtering in classes of dendritic neurons[13,18,22,33]. Therefore, the electrically distributed nature of central neurons suggests that voltage will not be controlled uniformly by a point-source voltage clamp[7,10,11]. Despite this, the somatic voltage clamp has become the method of choice to study synaptic physiology and neuronal excitability in central neurons because of the experimental tractability of obtaining electrical recordings from the soma using sharp microelectrode and whole-cell recording techniques *in vitro* and *in vivo*. Here, we have experimentally quantified errors in the somatic voltage clamp measurement of dendritic synapses.

Key to the measurement of the properties of synapses under voltage clamp is the control of the membrane potential at a fixed value through the time course of a synaptic conductance. Because of cable filtering, the ability of the somatic voltage clamp to control voltage at the site of activated dendritic synapses is expected to deteriorate with distance into the dendritic tree—the 'space clamp' problem[16]. However, it is not known how much of the dendritic tree is voltage clamped from the soma experimentally, and it is widely assumed that at least proximal dendritic synapses are accurately controlled[11]. Direct measurement shows that accurate control of membrane potential during simulated synaptic input is restricted to somatic and perisomatic sites, even when recordings are made at room temperature and the resting conductance pharmacologically reduced. Substantial escape from voltage clamp occurs at apical dendritic sites, with 50% of voltage control lost during a simulated fast excitatory synaptic conductance at just 60 µm from the soma at room temperature. Although the spatial control of membrane potential by the somatic voltage clamp was frequency dependent and marginally improved by experimental procedures such as recording at room temperature and reducing leak and resting conductance, voltage throughout the majority of the dendritic tree was uncontrolled even at steady state. Dendritic voltage escape will not only directly distort the somatic measurement of the properties of dendritic synaptic input, as shown here; in addition, by the recruitment of dendritic voltage-activated channels, dendritic voltage escape will further degrade the measurement of synaptic input in a manner dependent upon the dendritic expression pattern of voltage-activated ion channels[34]. We find at steady state that the amplitudes of voltage-command steps evoked at the soma under voltage clamp are heavily attenuated, with 50% attenuation apparent at 264 µm from the soma (**Supplementary Fig. 6** online). Therefore, in neocortical pyramidal neurons, the somatic voltage clamp cannot be used to describe the properties of dendritic voltage-activated conductances—an idea directly confirmed by the recording of the voltage influence of I_H at apical dendritic sites during the course of somatic voltage-command steps (**Figs. 2** and **6**). However, the somatic voltage clamp adequately controls the membrane potential at perisomatic sites and thus may be used to prevent the generation of action potential firing evoked by synaptic excitation. Moreover, the greater somato-dendritic control of voltage at steady state helps explain how sustained postsynaptic depolarization produced under somatic voltage clamp can provide sufficient dendritic depolarization to allow the induction of synaptic plasticity during pairing protocols[35].

In pyramidal neurons, the vast majority of excitatory synaptic contacts are made at the head of dendritic spines[36]. Therefore, voltage control at native synapses is likely to be poor because of the

compounding influence of spine neck resistance, a parameter not addressed in this study. Although a wide range of values have been reported for the resistance of the spine neck, which may reflect analysis of spines of different morphology[37–39], the concerted filtering properties of the dendritic shaft and spine neck, coupled with the fast time course of the synaptic conductance change mediated by the activation of spine head AMPA receptors[14], will ensure that even proximal dendritic synapses are poorly controlled by the somatic voltage clamp. Therefore, escape potentials generated within a dendritic spine may confound interpretation of experimental findings. For example, spine head voltage escape may allow the uncontrolled voltage-dependent coactivation of NMDA-type glutamate receptors[20] and/or the activation of spine voltage-activated calcium channels[40]. As calcium influx mediated by these channel classes has been shown to trigger biochemical events that ultimately lead to synaptic plasticity and the control of gene expression[41,42], the lack of dendritic voltage control may have unforeseen influence on synaptic and neuronal physiology.

The somatic voltage clamp inaccurately measures the amplitude and time course of dendritic synaptic conductance, with errors increasing as synaptic input is generated from progressively more distal dendritic sites. As the axon of a single presynaptic neuron typically makes multiple synaptic contacts with a postsynaptic cell at sites that can be distributed widely throughout the dendritic tree[43–45], the properties of a distributed single-axon synaptic input will be inaccurately measured by the somatic voltage clamp. Notably, our results suggest that when a distributed synapse is activated, somatic measurement errors will be compounded because of propagation delays and the distance-dependent slowing of the kinetics of unclamped dendritic synaptic potentials. Consequently, when synapses issued by a single axon are distributed in the dendritic tree, relatively distal synapses will not contribute to the peak of a somatically recorded synaptic current but instead will contribute at later times to prolong the time course of the current. Therefore, the influence of relatively remote synapses will not be considered when investigating the quantal properties of synaptic transmission, if synaptic currents are measured at times centered around the somatically recorded peak amplitude. Therefore, the lack of dendritic voltage control will have a direct impact on the recovery of key synaptic parameters such as quantal amplitude and the number of release sites[33,46]. Indeed, numerical simulation based simply on the somatic measurement of the peak amplitude of dendritic dEPSCs shows that quantal analysis, implemented using the mean-variance technique[47], accurately describes the number of release sites only when synaptic contacts are grouped at a given dendritic location, but markedly underestimates the number of release sites when synapses are dendritically distributed, either in groups or individually (**Supplementary Figs. 7** and **8** online; **Supplementary Methods** online). As this simulation did not take into account propagation delays, kinetic distortions or the effects of dendritic voltage escape, it is anticipated that such errors will be greater for native single-axon distributed synapses, unless synapses are positioned at electrotonically equivalent dendritic sites[48]. We find it interesting, therefore, that direct recording has shown severe dendro-somatic voltage attenuation of EPSPs generated at basal dendritic sites in neocortical pyramidal neurons[49]. Although the path length of basal dendrites is short compared to the apical dendrites of neocortical pyramidal neurons, the similar magnitude of EPSP attenuation[49] suggests that somatic voltage clamp errors will exist for synapses targeted to the basal dendritic tree. Furthermore, in the apical dendritic arbor of pyramidal neurons, synapses are often targeted to thin daughter dendrites, such as apical tuft and apical oblique dendrites. Frequency-dependent voltage attenuation in these fine-caliber dendrites[50] is likely to hinder the performance of the somatic voltage clamp even further.

Recently, the somatic voltage clamp has become a popular tool to study the dynamic behavior of neural circuits because of the ability to extract excitatory and inhibitory components from barrages of synaptic conductance generated during stimulus-evoked and spontaneous network activity[8,25,26,29–31]. However, when temporally overlapping excitatory and inhibitory synaptic inputs are generated at dendritic sites, the somatic voltage clamp underestimates the total synaptic conductance and inaccurately isolates excitatory and inhibitory components. Therefore, the total synaptic conductance received by a neuron during network activity has been underestimated by previous studies. During a barrage of synaptic activity, direct recording shows that errors in the separation and measurement of excitatory and inhibitory synaptic conductance are critically determined by the time-varying composition of the total synaptic conductance. It should be noted, however, that simulated excitatory and inhibitory inputs were generated at the same dendritic site, which replicates the anatomical arrangement of aligned excitatory and inhibitory synapses, a network design principle in the cortex[45]. This arrangement maximizes distortions generated by dendritic voltage escape. However, if excitatory and inhibitory input are not anatomically aligned but instead differentially targeted in the dendritic arbor, distance-dependent errors will directly affect the measurement of excitatory and inhibitory synaptic conductance. Therefore, the somatic voltage clamp will inaccurately measure the properties of synaptic conductance produced by the activation of spatially distinct assemblies of synapses engaged during different patterns of network behavior.

In summary, direct dendritic recording techniques have highlighted errors in the somatic voltage clamp measurement of dendritic synaptic input. All parameters of dendritic excitatory and inhibitory synaptic input are distorted in a dendritic distance–dependent manner. These measurement errors indicate that previous voltage clamp studies of dendritic neurons have described results heavily weighted by the measurement of proximal dendritic synapses and question the use of the somatic voltage clamp as a quantitative tool to study synaptic physiology in dendritic neurons.

METHODS

Brain slice preparation. Neocortical brain slices (300 μm) were prepared from Wistar rats (postnatal day (P) 25 to P36) following institutional and UK Home Office guidelines. Brain slices were maintained in a solution containing (in mM) 125 NaCl, 25 $NaHCO_3$, 3 KCl, 1.25 NaH_2PO_4, 2 $CaCl_2$, 1 $MgCl_2$, 3 sodium pyruvate, 25 glucose and 0.001 tetrodotoxin.

Electrophysiological recording. Triple whole-cell recordings were made from the soma and apical dendrite of layer 5B pyramidal neurons visualized under infrared differential interference contrast microscopy. In the majority of experiments, pipettes were filled with (in mM): 135 potassium gluconate, 7 NaCl, 10 HEPES, 2 disodium ATP, 0.3 sodium GTP, 2 $MgCl_2$ and 0.01 Alexa Fluor 568 (Molecular Probes) (pH 7.2–7.3; KOH). In some experiments, a cesium-rich intrapipette solution was used, containing (in mM) 130 or 135 CsCl, 5 or 1 EGTA, 10 HEPES, 2 disodium ATP, 0.3 sodium GTP, 2 $MgCl_2$ and 0.01 Alexa Fluor 568 (pH 7.2–7.3; CsOH). In the majority of experiments, antagonists of excitatory and inhibitory amino acid receptors were included in the extracellular medium (6-cyano-7-nitroquinoxaline-2,3-dione (10 μM); 6-imino-3-(4-methoxyphenyl)-1(6H)-pyridazinebutanoic acid hydrobromide (10 μM); D-(-)-2-amino-5-phosphonopentanoic acid (50 μM)). At the termination of each experiment, the location and morphology of neurons was examined by fluorescence microscopy and digitally recorded (Retiga EXI, QImaging). Somatic recording pipettes had a resistance of 3–6 MΩ, and pipettes for apical dendritic recordings, 10–12 MΩ. Somatic voltage clamp recordings were made with an Axopatch 200B amplifier (Molecular Devices). Series resistance was either uncompensated or compensated by >90% (prediction and correction) in

the presence of <10 μs lag. Two identical current clamp amplifiers (BVC-700A) were used to generate simulated synaptic input at either somatic or apical dendritic sites as changes of conductance using a real-time dynamic clamp[12,24]. Independent closely spaced pipettes positioned either at the soma or apical dendritic trunk sites were connected to amplifiers used to inject current and record membrane potential (10–570 μm from the soma; pipette separation, 6.6 ± 0.5 μm). Current and voltage signals were low-pass filtered (DC to 10 KHz) and acquired at 30–50 KHz. Data were acquired and analyzed using Axograph software (Molecular Devices). The voltage clamp holding voltage was set to the resting membrane potential (zero injected current; range, –60 to –68 mV under control conditions). The voltage clamp amplifier accurately reported the amplitude and time course of the synaptic current injected with the dynamic clamp system when connected to a model cell with an input resistance of 20 MΩ and time constant of 10 ms (**Supplementary Fig. 1**).

Barrages of simulated synaptic conductance were modeled as the sum of ten independent excitatory inputs and ten inhibitory inputs firing randomly at a mean frequency of 10 Hz (instantaneous frequencies were sampled from a bounded distribution of 0–250 Hz). Individual excitatory and inhibitory synaptic responses had the following properties: $E_{EPSC} = 0$ mV, $\tau_{rise} = 0.5$ ms, $\tau_{decay} = 5$ ms; $g_{EPSC} = 4.5$ nS; $E_{IPSC} = -80$ mV, $\tau_{rise} = 1$ ms, $\tau_{decay} = 10$ ms; $g_{IPSC} = 18$ nS. The properties of temporally overlapping excitatory and inhibitory synaptic conductance were calculated using linear regression analysis, where the slope and intercept of the current-voltage relationship recorded from the soma or from the site of synapse generation for each sample point across a somatic voltage range of 50 mV (5-mV steps). Excitatory and inhibitory components were separated according to methods detailed in ref. 25.

Statistical analysis. Data sets were compared with Student's *t*-test and current-voltage relationship fit by linear regression. All curve fitting was performed using Axograph. Values are expressed as mean ± s.e.m.

Note: Supplementary information is available on the Nature Neuroscience website.

ACKNOWLEDGMENTS

We are grateful to D. Hodgkin for encouragement. This work was supported by the Medical Research Council (UK).

AUTHOR CONTRIBUTIONS

S.R.W. performed all experiments and data analysis. S.J.M. performed quantal analysis simulations.

Published online at http://www.nature.com/natureneuroscience/
Reprints and permissions information is available online at http://npg.nature.com/reprintsandpermissions/

1. Hausser, M., Spruston, N. & Stuart, G.J. Diversity and dynamics of dendritic signaling. *Science* **290**, 739–744 (2000).
2. Johnston, D., Hablitz, J.J. & Wilson, W.A. Voltage clamp discloses slow inward current in hippocampal burst-firing neurones. *Nature* **286**, 391–393 (1980).
3. Finkel, A.S. & Redman, S.J. The synaptic current evoked in cat spinal motoneurones by impulses in single group 1a axons. *J. Physiol. (Lond.)* **342**, 615–632 (1983).
4. Blanton, M.G., Lo Turco, J.J. & Kriegstein, A.R. Whole cell recording from neurons in slices of reptilian and mammalian cerebral cortex. *J. Neurosci. Methods* **30**, 203–210 (1989).
5. Edwards, F.A., Konnerth, A. & Sakmann, B. Quantal analysis of inhibitory synaptic transmission in the dentate gyrus of rat hippocampal slices: a patch-clamp study. *J. Physiol. (Lond.)* **430**, 213–249 (1990).
6. Sakmann, B. & Neher, E. *Single-Channel Recording* (Plenum Press, New York, 1995).
7. Smith, T.G., Lecar, H., Redman, S.J. & Gage, P.W. *Voltage and Patch Clamping with Microelectrodes* (American Physiological Society, Bethesda, Maryland, 1984).
8. Borg-Graham, L.J., Monier, C. & Fregnac, Y. Visual input evokes transient and strong shunting inhibition in visual cortical neurons. *Nature* **393**, 369–373 (1998).
9. Johnston, D. & Brown, T.H. Interpretation of voltage-clamp measurements in hippocampal neurons. *J. Neurophysiol.* **50**, 464–486 (1983).
10. Spruston, N., Jaffe, D.B., Williams, S.H. & Johnston, D. Voltage- and space-clamp errors associated with the measurement of electrotonically remote synaptic events. *J. Neurophysiol.* **70**, 781–802 (1993).
11. Armstrong, C.M. & Gilly, W.F. Access resistance and space clamp problems associated with whole-cell patch clamping. *Methods Enzymol.* **207**, 100–122 (1992).
12. Williams, S.R. Spatial compartmentalization and functional impact of conductance in pyramidal neurons. *Nat. Neurosci.* **7**, 961–967 (2004).
13. Williams, S.R. & Stuart, G.J. Dependence of EPSP efficacy on synapse location in neocortical pyramidal neurons. *Science* **295**, 1907–1910 (2002).
14. Hausser, M. & Roth, A. Estimating the time course of the excitatory synaptic conductance in neocortical pyramidal cells using a novel voltage jump method. *J. Neurosci.* **17**, 7606–7625 (1997).
15. Williams, S.R. & Stuart, G.J. Role of dendritic synapse location in the control of action potential output. *Trends Neurosci.* **26**, 147–154 (2003).
16. Rall, W. Core conductor theory and cable properties of neurons. in *Handbook of Physiology - The Nervous System 1* (ed. Kandel, E.R.) 39–97 (American Physiological Society, Bethesada, Maryland, 1977).
17. Stuart, G. & Spruston, N. Determinants of voltage attenuation in neocortical pyramidal neuron dendrites. *J. Neurosci.* **18**, 3501–3510 (1998).
18. Magee, J.C. & Cook, E.P. Somatic EPSP amplitude is independent of synapse location in hippocampal pyramidal neurons. *Nat. Neurosci.* **3**, 895–903 (2000).
19. Sabatini, B.L. & Regehr, W.G. Timing of synaptic transmission. *Annu. Rev. Physiol.* **61**, 521–542 (1999).
20. Bekkers, J.M. & Stevens, C.F. NMDA and non-NMDA receptors are colocalized at individual excitatory synapses in cultured rat hippocampus. *Nature* **341**, 230–233 (1989).
21. Williams, S.R. & Stuart, G.J. Site independence of EPSP time course is mediated by dendritic Ih in neocortical pyramidal neurons. *J. Neurophysiol.* **83**, 3177–3182 (2000).
22. Berger, T., Larkum, M.E. & Luscher, H.R. High I(h) channel density in the distal apical dendrite of layer V pyramidal cells increases bidirectional attenuation of EPSPs. *J. Neurophysiol.* **85**, 855–868 (2001).
23. Kole, M.H., Hallermann, S. & Stuart, G.J. Single Ih channels in pyramidal neuron dendrites: properties, distribution, and impact on action potential output. *J. Neurosci.* **26**, 1677–1687 (2006).
24. Williams, S.R. & Stuart, G.J. Voltage- and site-dependent control of the somatic impact of dendritic IPSPs. *J. Neurosci.* **23**, 7358–7367 (2003).
25. Wehr, M. & Zador, A.M. Balanced inhibition underlies tuning and sharpens spike timing in auditory cortex. *Nature* **426**, 442–446 (2003).
26. Shu, Y., Hasenstaub, A. & McCormick, D.A. Turning on and off recurrent balanced cortical activity. *Nature* **423**, 288–293 (2003).
27. Pouille, F. & Scanziani, M. Enforcement of temporal fidelity in pyramidal cells by somatic feed-forward inhibition. *Science* **293**, 1159–1163 (2001).
28. Gabernet, L., Jadhav, S.P., Feldman, D.E., Carandini, M. & Scanziani, M. Somatosensory integration controlled by dynamic thalamocortical feed-forward inhibition. *Neuron* **48**, 315–327 (2005).
29. Cruikshank, S.J., Lewis, T.J. & Connors, B.W. Synaptic basis for intense thalamocortical activation of feedforward inhibitory cells in neocortex. *Nat. Neurosci.* **10**, 462–468 (2007).
30. Borg-Graham, L.J. The computation of directional selectivity in the retina occurs presynaptic to the ganglion cell. *Nat. Neurosci.* **4**, 176–183 (2001).
31. Hasenstaub, A., Sachdev, R.N. & McCormick, D.A. State changes rapidly modulate cortical neuronal responsiveness. *J. Neurosci.* **27**, 9607–9622 (2007).
32. Haider, B., Duque, A., Hasenstaub, A.R. & McCormick, D.A. Neocortical network activity *in vivo* is generated through a dynamic balance of excitation and inhibition. *J. Neurosci.* **26**, 4535–4545 (2006).
33. Jack, J.J., Kullmann, D.M., Larkman, A.U., Major, G. & Stratford, K.J. Quantal analysis of excitatory synaptic mechanisms in the mammalian central nervous system. *Cold Spring Harb. Symp. Quant. Biol.* **55**, 57–67 (1990).
34. Migliore, M. & Shepherd, G.M. Opinion: an integrated approach to classifying neuronal phenotypes. *Nat. Rev. Neurosci.* **6**, 810–818 (2005).
35. Liao, D., Hessler, N.A. & Malinow, R. Activation of postsynaptically silent synapses during pairing-induced LTP in CA1 region of hippocampal slice. *Nature* **375**, 400–404 (1995).
36. Harris, K.M. & Kater, S.B. Dendritic spines: cellular specializations imparting both stability and flexibility to synaptic function. *Annu. Rev. Neurosci.* **17**, 341–371 (1994).
37. Svoboda, K., Tank, D.W. & Denk, W. Direct measurement of coupling between dendritic spines and shafts. *Science* **272**, 716–769 (1996).
38. Bloodgood, B.L. & Sabatini, B.L. Neuronal activity regulates diffusion across the neck of dendritic spines. *Science* **310**, 866–869 (2005).
39. Araya, R., Jiang, J., Eisenthal, K.B. & Yuste, R. The spine neck filters membrane potentials. *Proc. Natl. Acad. Sci. USA* **103**, 17961–17966 (2006).
40. Sabatini, B.L. & Svoboda, K. Analysis of calcium channels in single spines using optical fluctuation analysis. *Nature* **408**, 589–593 (2000).
41. Kennedy, M.B., Beale, H.C., Carlisle, H.J. & Washburn, L.R. Integration of biochemical signaling in spines. *Nat. Rev. Neurosci.* **6**, 423–434 (2005).
42. Zhang, S.J. *et al.* Decoding NMDA receptor signaling: identification of genomic programs specifying neuronal survival and death. *Neuron* **53**, 549–562 (2007).
43. Redman, S. & Walmsley, B. The time course of synaptic potentials evoked in cat spinal motoneurones at identified group Ia synapses. *J. Physiol. (Lond.)* **343**, 117–133 (1983).
44. Buhl, E.H., Halasy, K. & Somogyi, P. Diverse sources of hippocampal unitary inhibitory postsynaptic potentials and the number of synaptic release sites. *Nature* **368**, 823–828 (1994).
45. Somogyi, P., Tamas, G., Lujan, R. & Buhl, E.H. Salient features of synaptic organization in the cerebral cortex. *Brain Res. Brain Res. Rev.* **26**, 113–135 (1998).
46. Redman, S. Quantal analysis of synaptic potentials in neurons of the central nervous system. *Physiol. Rev.* **70**, 165–198 (1990).
47. Silver, R.A., Momiyama, A. & Cull-Candy, S.G. Locus of frequency-dependent depression identified with multiple-probability fluctuation analysis at rat climbing fibre–Purkinje cell synapses. *J. Physiol. (Lond.)* **510**, 881–902 (1998).
48. Silver, R.A., Lubke, J., Sakmann, B. & Feldmeyer, D. High-probability uniquantal transmission at excitatory synapses in barrel cortex. *Science* **302**, 1981–1984 (2003).
49. Nevian, T., Larkum, M.E., Polsky, A. & Schiller, J. Properties of basal dendrites of layer 5 pyramidal neurons: a direct patch-clamp recording study. *Nat. Neurosci.* **10**, 206–214 (2007).
50. Jaffe, D.B. & Carnevale, N.T. Passive normalization of synaptic integration influenced by dendritic architecture. *J. Neurophysiol.* **82**, 3268–3285 (1999).